Nuclear Science and Techniques (2024) 35:161
https://doi.org/10.1007/s41365-024-01542-x

Possibility of reaching the predicted center of the “island of stability” via the radioactive beam-induced fusion reactions

Ming-Hao Zhang[1,2] · **Ying Zou**[1,2] · **Mei-Chen Wang**[1,2] · **Gen Zhang**[3] · **Qing-Lin Niu**[1,2] · **Feng-Shou Zhang**[1,2,4]

Received: 6 May 2024 / Revised: 12 June 2024 / Accepted: 15 June 2024 / Published online: 4 September 2024
© The Author(s), under exclusive licence to China Science Publishing & Media Ltd. (Science Press), Shanghai Institute of Applied Physics, the Chinese Academy of Sciences, Chinese Nuclear Society 2024

Abstract

Based on the dinuclear system model, the synthesis of the predicted double-magic nuclei ^{298}Fl and ^{304}120 was investigated via neutron-rich radioactive beam-induced fusion reactions. The reaction ^{58}Ca + ^{244}Pu is predicted to be favorable for producing ^{298}Fl with a maximal ER cross section of 0.301 pb. Investigations of the entrance channel effect reveal that the ^{244}Pu target is more promising for synthesizing ^{298}Fl than the neutron-rich targets ^{248}Cm and ^{249}Bk, because of the influence of the Coulomb barrier. For the synthesis of ^{304}120, the maximal ER cross section of 0.046 fb emerges in the reaction ^{58}V + ^{249}Bk, indicating the need for further advancements in both experimental facilities and reaction mechanisms.

Keywords Superheavy nuclei · Dinuclear system model · Fusion reaction · Double-magic nucleus · Radioactive beam

1 Introduction

As the center of the “island of stability” was predicted to be at $Z = 114$ and $N = 184$ by the macroscopic–microscopic model [1–5], reaching the next shell closure has been a major goal in nuclear physics. Various theoretical methods, including the Skyrme–Hartree–Fock approach and relativistic mean-field model, have predicted the proton and neutron shells at $Z = 114$, 120, 124, or 126 and $N = 184$ [3–13]. In recent years, superheavy elements with proton numbers up to $Z = 118$ have been synthesized via fusion reactions [14–25], along with the discovery of many new superheavy nuclei [26–33]. Despite these achievements, the neutron-rich superheavy nuclei region remains unknown.

The existence of superheavy nuclei with $Z \geq 104$ is mainly attributed to shell-structure effects. This information has led to the investigation of superheavy isotopes near the shell closure. Nevertheless, the experimental feasibility to the “island of stability” via the stable beam-induced hot fusion reactions encounters challenges due to the limited availability of actinide target materials and the low neutron-to-proton ratio in the stable projectiles. Consequently, alternative approaches, including multinucleon transfer and radioactive-induced fusion reactions, have been proposed. Nowadays, modern radioactive beam accelerators, such as the Radioactive Isotope Beam Factory (RIBF), Heavy Ion Research Facility in Lanzhou (HIRFL), Facility for Rare Isotope Beams (FRIB) and Second-generation System On-line Production of Radioactive Ions (SPIRAL2) [34–37], have been developed, offering new opportunities to explore the “island of stability” via radioactive-beam-induced reactions in future experiments.

To describe the heavy-ion collision mechanisms, several macroscopic [38–45] and microscopic models [46–54] were developed and examined. One of the macroscopic models, the dinuclear system (DNS) model, is proved to be a reliable

This work was supported by the National Key R&D Program of China (No. 2023YFA1606401), the National Natural Science Foundation of China (Nos. 12135004, 11635003 and 11961141004) and the Guangxi Natural Science Foundation (No. 2022GXNSFBA035549).

✉ Feng-Shou Zhang
fszhang@bnu.edu.cn

1 The Key Laboratory of Beam Technology of Ministry of Education, School of Physics and Astronomy, Beijing Normal University, Beijing 100875, China

2 Institute of Radiation Technology, Beijing Academy of Science and Technology, Beijing 100875, China

3 School of Physical Science and Technology, Guangxi University, Nanning 530004, China

4 Center of Theoretical Nuclear Physics, National Laboratory of Heavy Ion Accelerator of Lanzhou, Lanzhou 730000, China

theoretical tool for describing the fusion-evaporation reactions [8, 55–74]. In this study, the optimal reaction systems and the corresponding incident energies for the synthesis of the predicted double magic nuclei $^{298}_{184}$Fl and $^{304}_{184}$120 via fusion reactions with radioactive beams were investigated using the DNS model.

The remainder of this article is organized as follows: In Sect. 2, the theoretical details of the DNS model are provided, followed by an evaluation of the reliability of the model using the experimental results of the evaporation residue (ER) cross sections of the fusion reactions ^{48}Ca + ^{242}Pu and ^{48}Ca + ^{244}Pu. In Sect. 3, the synthesis of the predicted double magic nucleus ^{298}Fl employing neutron-rich radioactive projectiles and the ^{244}Pu, ^{248}Cm, and ^{249}Bk targets is explored, and the entrance channel effect is discussed. In addition, radioactive-beam-induced reactions for the synthesis of the predicted double magic nucleus ^{304}120 based on the ^{248}Cm, ^{249}Bk, and ^{249}Cf targets were also investigated. Section 4 presents the conclusions of this study.

2 Theoretical descriptions

Within the framework of the DNS model, the process of forming the superheavy nucleus is divided into capture, fusion, and survival stages, and the expression of the corresponding ER cross section can be written as

$$\sigma_{\mathrm{ER}}(E_{\mathrm{c.m.}}) = \frac{\pi\hbar^2}{2\mu E_{\mathrm{c.m.}}} \sum_J (2J+1) T(E_{\mathrm{c.m.}}, J) \times P_{\mathrm{CN}}(E_{\mathrm{c.m.}}, J) W_{\mathrm{sur}}(E_{\mathrm{c.m.}}, J), \tag{1}$$

$T\left(E_{\mathrm{c.m.}}, J\right)$ is the transmission probability of colliding partners overcoming the Coulomb barrier and forming a DNS. $P_{\mathrm{CN}}\left(E_{\mathrm{c.m.}}, J\right)$ is the fusion probability at which the projectile nucleon is transferred to the target, thereby forming a compound nucleus [75]. $W_{\mathrm{sur}}\left(E_{\mathrm{c.m.}}, J\right)$ denotes the survival probability when the compound nucleus undergoes de-excitation via neutron emission rather than fission [76].

The expression for the capture cross section σ_{cap} is as follows [58]:

$$\sigma_{\mathrm{cap}}\left(E_{\mathrm{c.m.}}\right) = \frac{\pi\hbar^2}{2\mu E_{\mathrm{c.m.}}} \sum_J (2J+1) T\left(E_{\mathrm{c.m.}}, J\right), \tag{2}$$

where transmission probability is defined as follows:

$$T\left(E_{\mathrm{c.m.}}, J\right) = \int f(B) T\left(E_{\mathrm{c.m.}}, B, J\right) \mathrm{d}B, \tag{3}$$

here $T(E_{\mathrm{c.m.}}, B, J)$ follows Ahmed's formula [77–79]: The parameters of the asymmetric barrier distribution $f(B)$ are adopted from Ref. [80]. The interaction potential of the colliding nuclei is defined as [58]

$$V(R, \beta_1, \beta_2, \theta_1, \theta_2) = \frac{1}{2} C_1 (\beta_1 - \beta_1^0)^2 + \frac{1}{2} C_2 (\beta_2 - \beta_2^0)^2 + V_{\mathrm{C}}(R, \beta_1, \beta_2, \theta_1, \theta_2) + V_{\mathrm{N}}(R, \beta_1, \beta_2, \theta_1, \theta_2), \tag{4}$$

where $C_{1,2}$ denotes the nuclear surface stiffness [81]. $\beta_{1,2}$ and $\beta_{1,2}^0$ represent the dynamic quadrupole deformation and static deformation of the projectile and target nucleus, respectively. The Coulomb potential V_{C} is given by the Wong formula [82], and the nuclear potential V_{N} is described using the double-folding potential [83].

When the DNS evolves into a compound nucleus, the nucleon transfer process is driven by the driving potential along the degree of mass asymmetry $\eta = \left(A_1 - A_2\right) / \left(A_1 + A_2\right)$ [58]. The distribution probability of fragments $P\left(Z_1, N_1, E_1, t\right)$ can be obtained by solving the following set of master equations:

$$\begin{aligned} \frac{\mathrm{d}P(Z_1, N_1, E_1, t)}{\mathrm{d}t} &= \sum_{Z_1'} W_{Z_1, N_1; Z_1', N_1}(t) \times [d_{Z_1, N_1} P(Z_1', N_1, E_1, t) - d_{Z_1', N_1} P(Z_1, N_1, E_1, t)] \\ &+ \sum_{N_1'} W_{Z_1, N_1; Z_1, N_1'}(t) \times [d_{Z_1, N_1} P(Z_1, N_1', E_1, t) - d_{Z_1, N_1'} P(Z_1, N_1, E_1, t)] \\ &- [\Lambda_{\mathrm{qf}}(\Theta(t)) + \Lambda_{\mathrm{fis}}(\Theta(t))] P(Z_1, N_1, E_1, t). \end{aligned} \tag{5}$$

Here $W_{Z_1, N_1; Z_1', N_1}$ denotes the mean transition probability between state (Z_1, N_1) and (Z_1', N_1) [84], with d_{Z_1, N_1} representing the microscopic dimension. The likelihood of the DNS decaying via quasi-fission and the probability of heavy fragment fission are denoted by the quasi-fission probability Λ_{qf} and the fission probability Λ_{fis}, which are determined using the one-dimensional Kramers formula [85].

The complete fusion process within the DNS requires overcoming the inner fusion barrier B_{fus}, which originates from the potential energy difference between the incident point and the B.G. point [86]. Thus, the fusion probability can be obtained by adding the distribution probabilities that overcome the inner fusion barrier.

$$P_{\mathrm{CN}}(E_{\mathrm{c.m.}}, J) = \sum_{Z_1=1}^{Z_{\mathrm{B.G.}}} \sum_{N_1=1}^{N_{\mathrm{B.G.}}} P(Z_1, N_1, E_1, \tau_{\mathrm{int}}(J)), \tag{6}$$

where the interaction time $\tau_{\mathrm{int}}(J)$ is estimated using the deflection function method [87].

During the survival stage, the excited compound nucleus is unstable and undergoes light particle emission or fission to reach the ground stage. The survival probability for neutron emission competing with fission at excitation energy E^*_{CN} is calculated as

$$W_{\mathrm{sur}}(E^*_{\mathrm{CN}}, x, J) = P(E^*_{\mathrm{CN}}, x, J) \prod_{i=1}^{x} \left[\frac{\Gamma_{\mathrm{n}}(E^*_i, J)}{\Gamma_{\mathrm{n}}(E^*_i, J) + \Gamma_{\mathrm{f}}(E^*_i, J)} \right]. \tag{7}$$

$P(E^*_{\mathrm{CN}}, x, J)$ denotes the realization probability that the compound nucleus evaporates x neutrons [88]. The partial decay width for neutron evaporation Γ_{n} and the fission decay width Γ_{f} were determined using the Weisskopf–Ewing theory [89] and the Bohr–Wheeler transition-state method [90], with the level density given by the standard Fermi gas model [91]. The fission barrier is defined as:

$$\begin{aligned} B_{\mathrm{f}}(E^*_i, J) = {} & B^{\mathrm{LD}}_{\mathrm{f}}\left(1 - x_{\mathrm{LD}} T_i^2\right) \\ & + B^{\mathrm{M}}_{\mathrm{f}}(E^*_i = 0) \exp\left(-\frac{E^*_i}{E_{\mathrm{D}}}\right) \\ & - \left(\frac{\hbar^2}{2J_{\mathrm{g.s.}}} - \frac{\hbar^2}{2J_{\mathrm{s.d.}}}\right) J(J+1), \end{aligned} \tag{8}$$

here E^*_i represents the excitation energy prior to the emission of the ith neutron. ${B_{\mathrm{f}}}^{\mathrm{LD}}$ is the macroscopic part determined by the liquid-drop model and ${B_{\mathrm{f}}}^{\mathrm{M}}$ represents the microscopic shell correction [1]. x_{LD} is a temperature dependent parameter [91]. The range of shell damping energy E_{D} introduces theoretical uncertainties [64, 92, 93], indicating an excitation-energy-dependent shell effect. $J_{\mathrm{g.s.}}$ and $J_{\mathrm{s.d.}}$ denote the moments of inertia of the compound nucleus in its ground state and saddle point, respectively, [94, 95].

Based on the ample experimental results obtained from the reactions ${}^{48}\mathrm{Ca} + {}^{242}\mathrm{Pu} \rightarrow {}^{290-xn}\mathrm{Fl} + xn$ and ${}^{48}\mathrm{Ca} + {}^{244}\mathrm{Pu} \rightarrow {}^{292-xn}\mathrm{Fl} + xn$, the reliability of the DNS model has been evaluated, as illustrated in Fig. 1. For the majority of the experimental data, the calculated ER cross sections are in good agreement within the error margin. This consistency supports the reliability of the DNS model for identifying the optimal reaction systems and the corresponding incident energies for producing new superheavy nuclei through fusion reactions.

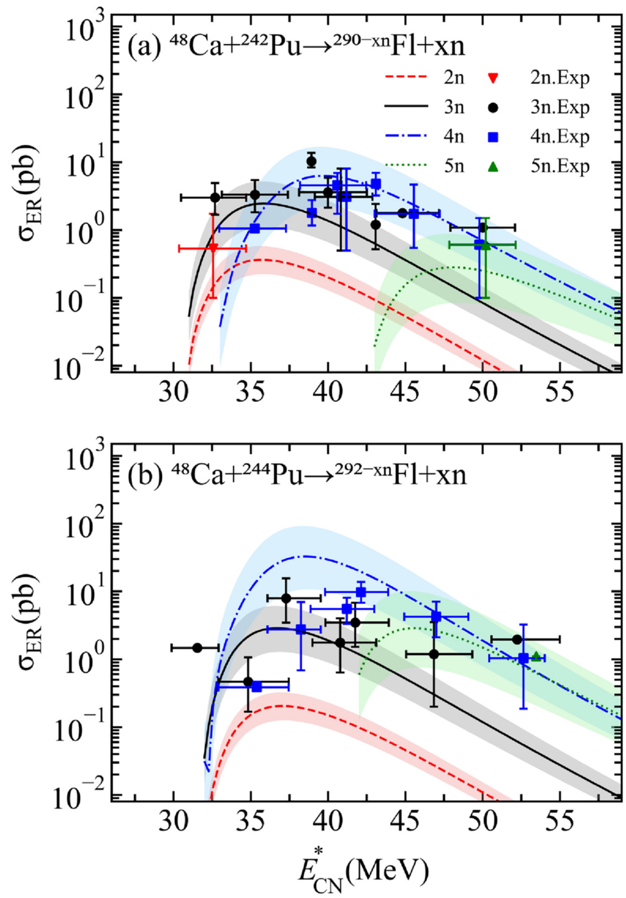

Fig. 1 (Color online) Comparison of the calculated results with the available experimental data from the reactions ${}^{48}\mathrm{Ca} + {}^{242,244}\mathrm{Pu}$ [98–103]. The calculation uncertainties are given by the shaded areas

3 Results and discussion

3.1 The synthesis of the predicted double-magic nucleus ^{298}Fl with the ^{244}Pu target

Many Fl isotopes have been synthesized via hot fusion reactions using Pu targets [96–103]. Among the available Pu targets, the neutron-rich ^{244}Pu target has emerged as a promising candidate for achieving the next shell closure, $N = 184$. Through hot fusion reactions with the ^{244}Pu target and radioactive projectiles ^{56,57,58}Ca, the synthesis of the double-magic nucleus ^{298}Fl predicted by the macroscopic–microscopic model is investigated.

For the reaction ${}^{56}\mathrm{Ca} + {}^{244}\mathrm{Pu} \rightarrow {}^{298}\mathrm{Fl} + 2\mathrm{n}$, the predicted maximal ER cross section of 0.0005 pb which calculated by DNS model, is significantly below the detection limitation. In contrast, the ER cross sections for the reactions ${}^{57}\mathrm{Ca} + {}^{244}\mathrm{Pu} \rightarrow {}^{298}\mathrm{Fl} + 3\mathrm{n}$ and ${}^{58}\mathrm{Ca} + {}^{244}\mathrm{Pu} \rightarrow {}^{298}\mathrm{Fl} + 4\mathrm{n}$ are presented in Fig. 2. The maximal ER cross section for the latter reaction reaches 0.301 pb, which is approximately an order of magnitude higher than that 0.044 pb for the reaction ${}^{57}\mathrm{Ca} + {}^{244}\mathrm{Pu} \rightarrow {}^{298}\mathrm{Fl} + 3\mathrm{n}$. It is observed that the predicted maximal ER cross sections for the reactions induced by radioactive Ca beams are suppressed when compared to those induced by ^{48}Ca. To further investigate this phenomenon, the capture, fusion and survival stages of the reactions ${}^{48}\mathrm{Ca} + {}^{244}\mathrm{Pu} \rightarrow {}^{288}\mathrm{Fl} + 4\mathrm{n}$ and ${}^{58}\mathrm{Ca} + {}^{244}\mathrm{Pu} \rightarrow {}^{298}\mathrm{Fl} + 4\mathrm{n}$ are investigated in Fig. 3.

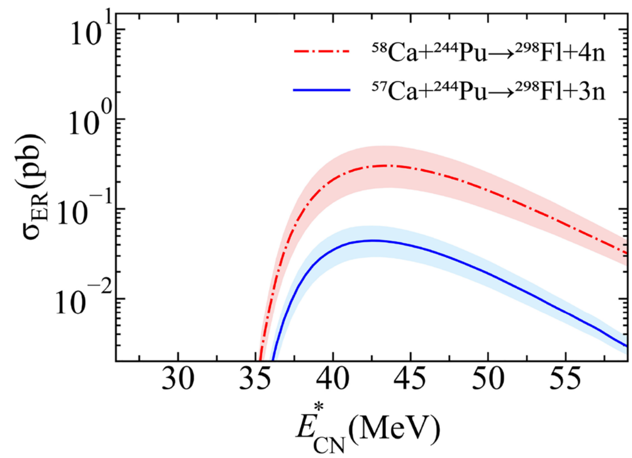

Fig. 2 (Color online) The calculated ER cross sections for the reactions $^{57}Ca + {}^{244}Pu \rightarrow {}^{298}Fl + 3n$ and $^{58}Ca + {}^{244}Pu \rightarrow {}^{298}Fl + 4n$. The calculation uncertainties are given by the shaded areas

Figure 3a shows the calculated capture cross sections for the reactions $^{48,58}Ca + {}^{244}Pu$ alongside the experimental data of the reaction $^{48}Ca + {}^{244}Pu$. It reveals an increasing trend for the capture cross sections with increasing E^*_{CN}, which can be attributed to the enhanced probability of the colliding nuclei overcoming the Coulomb barrier at elevated E^*_{CN}. The alignment between the calculated and experimental results for the reaction $^{48}Ca + {}^{244}Pu$ supports the predictive ability of the empirical coupled channel model. For the reaction $^{58}Ca + {}^{244}Pu$, the excitation energy of the Coulomb barrier $V_B + Q$ is 42.4 MeV. This value is approximately 8.3 MeV higher than that of the reaction $^{48}Ca + {}^{244}Pu$, which is 34.1 MeV. Consequently, such a significant increase in the $V_B + Q$ value for the ^{58}Ca-induced reaction leads to a suppressed capture cross section at low E^*_{CN}.

In Fig. 3b, the fusion probabilities for the reactions $^{48,58}Ca + {}^{244}Pu$ are depicted. The fusion probability exhibited an upward trend with increasing E^*_{CN}, which is ascribed to the increased likelihood of overcoming the inner fusion barrier at a high E^*_{CN}. Notably, the fusion probability of the reaction $^{58}Ca + {}^{244}Pu$ was lower than that for the reaction $^{48}Ca + {}^{244}Pu$. This difference is primarily due to variations in the inner fusion barrier, which are influenced by the mass asymmetry of the reaction system. A further analysis is shown in Fig. 4 elaborates on the influence of the driving potential in the fusion process. This reveals that the lower mass asymmetry of reaction $^{58}Ca + {}^{244}Pu$ results in an incident point substantially distant from the B.G. point. Consequently, the inner fusion barrier for the reaction $^{58}Ca + {}^{244}Pu$ is 13.1 MeV, which is significantly higher than that for the reaction $^{48}Ca + {}^{244}Pu$ (9.4 MeV). This marked difference in the inner fusion barriers accounts for the observed suppression of the fusion probability for the reaction $^{58}Ca + {}^{244}Pu$ in Fig. 3b,

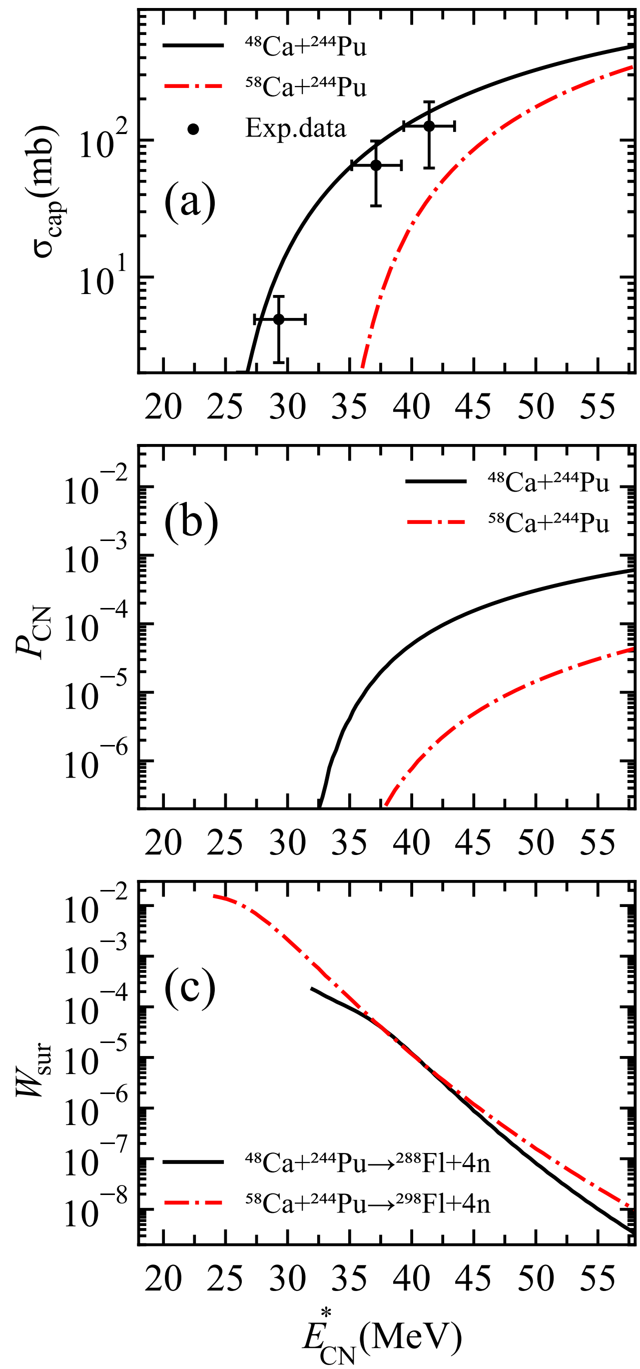

Fig. 3 (Color online) **a** The calculated capture cross sections, **b** fusion probabilities and **c** survival probabilities of the reactions $^{48}Ca + {}^{244}Pu \rightarrow {}^{288}Fl + 4n$ (black solid lines) and $^{58}Ca + {}^{244}Pu \rightarrow {}^{298}Fl + 4n$ (red dash-dot lines). The experimental values for the reaction $^{48}Ca + {}^{244}Pu$ are denoted by the black circles [104]

revealing the crucial role of mass asymmetry in influencing the formation of the compound nucleus in the fusion process.

Figure 3c illustrates the survival probabilities for the formation of nuclei ^{288}Fl and ^{298}Fl via the 4n-emission channel.

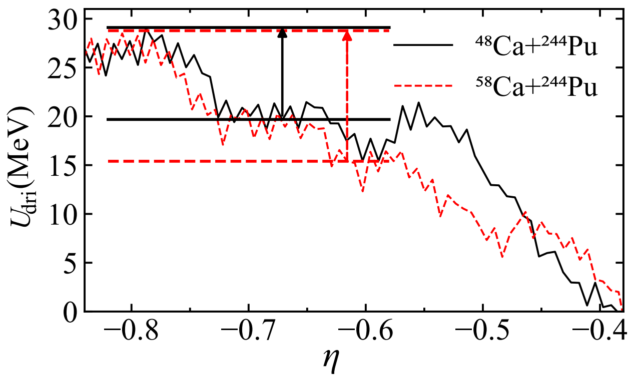

Fig. 4 (Color online) The driving potential as a function of mass asymmetry for the reactions $^{48,58}Ca + {}^{244}Pu$. The entrance channels of the reactions $^{48}Ca + {}^{244}Pu$ and $^{58}Ca + {}^{244}Pu$ are represented by the black solid line arrow and the red dashed line arrow

The survival probability of the nucleus ^{298}Fl was observed to be slightly higher than that of ^{288}Fl. However, fission became the dominant de-excitation mode at high E^*_{CN}, which leads to a downward trend in the survival probabilities. Consequently, the disparity in survival probabilities diminishes in the high E^*_{CN} region. This decline in the survival probability at elevated E^*_{CN}, coupled with the suppression of the capture and fusion probabilities, results in a reduced maximal ER cross section for the synthesis of ^{298}Fl using radioactive Ca projectiles in comparison with the Fl isotopes produced with the ^{48}Ca beam.

3.2 The synthesis of the predicted double-magic nucleus ^{298}Fl with the ^{248}Cm and ^{249}Bk targets

Among the experimentally accessible actinide targets, ^{248}Cm and ^{249}Bk, which have a neutron number of 152, are the most neutron-rich target materials currently available for fusion reactions aimed at exploring the neutron-rich superheavy nuclei region. Table 1 presents the maximal ER cross sections for the synthesis of the double-magic nucleus ^{298}Fl through fusion reactions using ^{248}Cm and ^{249}Bk targets and radioactive projectiles $^{52-54}$Ar and ^{51,52}Cl, in comparison with reactions involving the ^{244}Pu target. The maximal ER cross section for a ^{248}Cm-based reaction is 0.129 pb for the reaction $^{54}Ar + {}^{248}Cm \rightarrow {}^{298}Fl + 4n$. In contrast, for the ^{249}Bk-based reactions, the maximal ER cross section achieved with the heaviest known ^{52}Cl projectile was approximately 0.004 pb.

Despite the higher number of neutrons in the ^{248}Cm and ^{249}Bk targets, Table 1 suggests that the maximal ER cross sections achieved by these targets do not present a clear advantage over those achieved by the ^{244}Pu-based reactions. Further examination of the entrance channel effects is shown in Fig. 5, which includes the capture cross sections, fusion probabilities and ER cross sections for the reactions $^{53}Ar + {}^{248}Cm \rightarrow {}^{298}Fl + 3n$ and $^{52}Cl + {}^{249}Bk \rightarrow {}^{298}Fl + 3n$. High $V_B + Q$ values for the reactions $^{53}Ar + {}^{248}Cm$ (46.9 MeV) and $^{52}Cl + {}^{249}Bk$

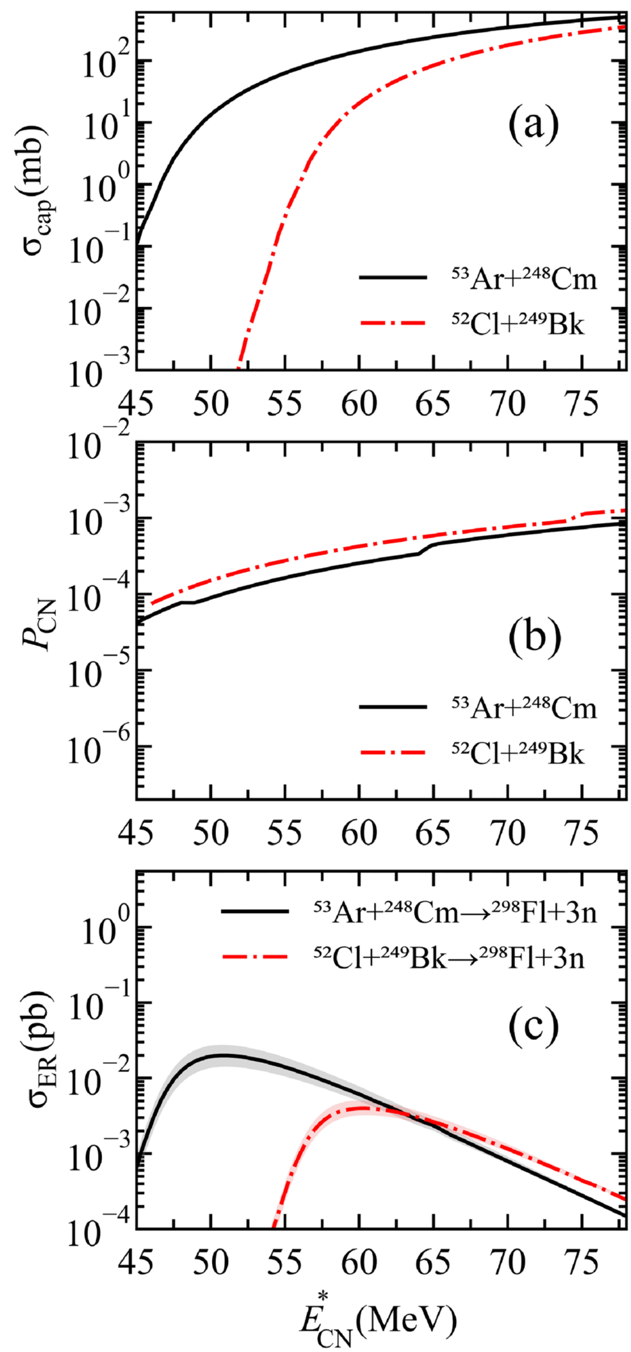

Fig. 5 (Color online) **a** The calculated capture cross sections, **b** fusion probabilities and **c** ER cross sections of the reactions $^{53}Ar + {}^{248}Cm \rightarrow {}^{298}Fl + 3n$ and $^{52}Cl + {}^{249}Bk \rightarrow {}^{298}Fl + 3n$. The calculation uncertainties are given by the shaded areas

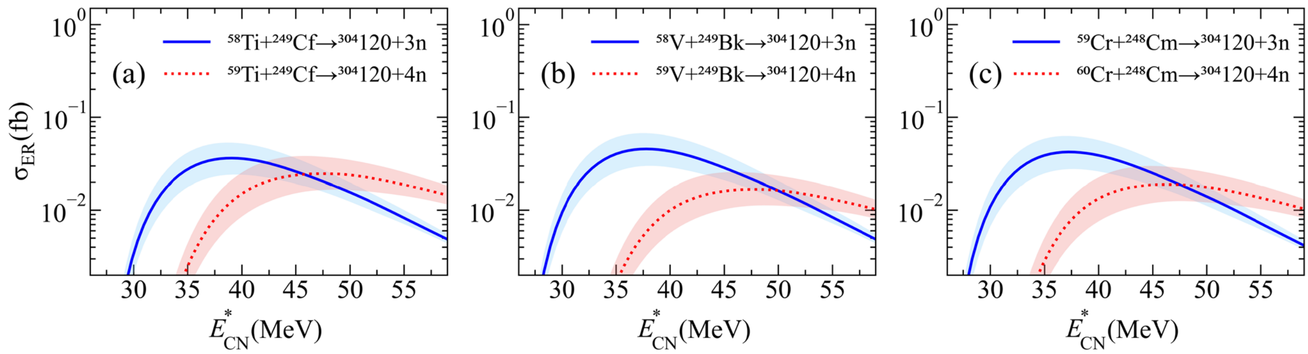

Fig. 6 (Color online) The predicted ER cross sections for the reactions **a** ^{58}Ti + ^{249}Cf → ^{304}120 + 3n, ^{59}Ti + ^{249}Cf → ^{304}120 + 4n, **b** ^{60}Cr + ^{249}Bk → ^{304}120 + 3n, ^{59}V + ^{249}Bk → ^{304}120 + 4n and **c** ^{59}Cr + ^{248}Cm → ^{304}120 + 3n, ^{60}Cr + ^{248}Cm → ^{304}120 + 4n. The calculation uncertainties are given by the shaded areas

Table 1 The predicted maximal ER cross sections, the corresponding optimal incident energy $E_{c.m.}$ and the E^*_{CN} of the radioactive-beam-induced reactions for producing the predicted double-magic nucleus ^{298}Fl

Reaction	$E_{c.m.}$ (MeV)	E^*_{CN} (MeV)	σ^{max}_{ER} (pb)
^{244}Pu (^{58}Ca,4n) ^{298}Fl	189.8	43.0	$0.301^{+0.204}_{-0.130}$
^{248}Cm (^{54}Ar,4n) ^{298}Fl	178.5	53.0	$0.129^{+0.070}_{-0.046}$
^{244}Pu (^{57}Ca,3n) ^{298}Fl	191.2	43.0	$0.044^{+0.021}_{-0.015}$
^{248}Cm (^{53}Ar,3n) ^{298}Fl	178.8	51.0	$0.020^{+0.008}_{-0.006}$
^{249}Bk (^{52}Cl,3n) ^{298}Fl	170.3	60.0	$0.004^{+0.001}_{-0.001}$
^{244}Pu (^{56}Ca,2n) ^{298}Fl	194.3	44.0	$0.0005^{+0.0002}_{-0.0001}$
^{248}Cm (^{52}Ar,2n) ^{298}Fl	180.0	49.0	$0.0003^{+0.00008}_{-0.00006}$
^{249}Bk (^{51}Cl,2n) ^{298}Fl	170.3	57.0	$0.0001^{+0.00002}_{-0.00002}$

Table 2 The same as in Table 1, but for producing the predicted double-magic nucleus ^{304}120

Reaction	$E_{c.m.}$ (MeV)	E^*_{CN} (MeV)	σ^{max}_{ER} (fb)
^{249}Bk (^{58}V, 3n) ^{304}120	237.1	38.0	$0.046^{+0.022}_{-0.016}$
^{248}Cm (^{59}Cr, 3n) ^{304}120	246.3	37.0	$0.042^{+0.021}_{-0.015}$
^{249}Cf (^{58}Ti, 3n) ^{304}120	229.8	39.0	$0.036^{+0.017}_{-0.012}$
^{249}Cf (^{59}Ti, 4n) ^{304}120	230.0	47.0	$0.025^{+0.014}_{-0.008}$
^{248}Cm (^{60}Cr, 4n) ^{304}120	255.2	46.0	$0.019^{+0.011}_{-0.006}$
^{249}Bk (^{59}V, 4n) ^{304}120	245.4	48.0	$0.017^{+0.009}_{-0.005}$
^{248}Cm (^{58}Cr, 2n) ^{304}120	246.2	36.0	$0.008^{+0.003}_{-0.002}$
^{249}Bk (^{57}V, 2n) ^{304}120	237.0	37.0	$0.008^{+0.002}_{-0.002}$
^{249}Cf (^{57}Ti, 2n) ^{304}120	227.5	38.0	$0.006^{+0.002}_{-0.001}$

(56.2 MeV) significantly suppress the capture cross sections for these reactions as depicted in Fig. 5a, in comparison with the reaction ^{58}Ca + ^{244}Pu in Fig. 3a.

During the fusion process, as illustrated in Fig. 5b, the fusion probability for the reaction ^{52}Cl + ^{249}Bk is slightly higher than that for the reaction ^{53}Ar + ^{248}Cm, owing to the relatively higher mass asymmetry of the ^{52}Cl + ^{249}Bk reaction. It can be observed that the high mass asymmetry values contribute to the fusion probabilities for these reactions, surpassing that of the reaction ^{58}Ca + ^{244}Pu in Fig. 3b. Despite the enhancement in the fusion stage, the maximal ER cross sections for synthesizing ^{298}Fl remain suppressed in reactions based on ^{248}Cm and ^{249}Bk targets in Fig. 5c, primarily due to the reduced capture cross sections. Note that ^{58}Ca is a weakly bound nucleus. The complex structure and low binding energy of ^{58}Ca may lead to neutron evaporation or projectile breakup, potentially suppressing the ER cross section.

3.3 Investigations on the synthesis of the predicted double-magic nucleus ^{304}120

For the synthesis of the double-magic nucleus ^{304}120 predicted by the relativistic mean-field model, the reaction systems employing the radioactive projectiles and the experimentally accessible heavy actinide targets ^{249}Cf, ^{249}Bk and ^{248}Cm are investigated. The calculated maximal ER cross sections and corresponding incident energies for these reactions to synthesize ^{304}120 are presented in Table 2. This reveals that among the investigated reaction systems, the highest maximal ER cross section of 0.046 fb emerges in the reaction ^{58}V + ^{249}Bk → ^{304}120 + 3n.

Figure 6 further illustrates the ER cross sections for the reactions ^{58}Ti + ^{249}Cf → ^{304}120 + 3n, ^{59}Ti + ^{249}Cf → ^{304}120 + 4n, ^{58}V + ^{249}Bk → ^{304}120 + 3n, ^{59}V + ^{249}Bk → ^{304}120 + 4n, ^{59}Cr + ^{248}Cm → ^{304}120 + 3n, ^{60}Cr + ^{248}Cm → ^{304}120 + 4n. It can be found that the 3n-emission channel is promising for the synthesis of ^{304}120. Nevertheless, the maximal ER cross sections are approximately 10^{-2} femtobarns, which is significantly lower than the current detection capabilities. Therefore, the advancement of experimental methodologies is required, including the development of more experimentally feasible neutron-rich radioactive projectiles, enhancement of radioactive beam intensities, improvement of detection techniques, and exploration of alternative reaction mechanisms such as multinucleon transfer reactions. These approaches are critical for reaching the center of the predicted "island of stability".

4 Summary

In this study, a comprehensive investigation of radioactive-beam-induced fusion reactions was conducted to approach the center of the predicted "island of stability". By employing radioactive projectiles $^{56-58}$Ca, $^{52-54}$Ar and ^{51,52}Cl combining with the ^{244}Pu, ^{248}Cm and ^{249}Bk targets, the synthesis of the predicted double-magic nucleus ^{298}Fl is investigated. The maximal ER cross section of 0.301 pb appears in the reaction $^{58}\mathrm{Ca} + {}^{244}\mathrm{Pu} \to {}^{298}\mathrm{Fl} + 4\mathrm{n}$. The capture, fusion and survival stages are discussed for the reactions $^{48}\mathrm{Ca} + {}^{244}\mathrm{Pu} \to {}^{288}\mathrm{Fl} + 4\mathrm{n}$ and $^{58}\mathrm{Ca} + {}^{244}\mathrm{Pu} \to {}^{298}\mathrm{Fl} + 4\mathrm{n}$, revealing that the critical influence of the Coulomb barrier and mass asymmetry results in the reduced maximal ER cross section for the reaction $^{58}\mathrm{Ca} + {}^{244}\mathrm{Pu} \to {}^{298}\mathrm{Fl} + 4\mathrm{n}$. The effects of the entrance channel were also investigated, indicating that the ^{244}Pu target is more promising than the neutron-rich ^{248}Cm and ^{249}Bk targets for synthesizing the nucleus ^{298}Fl, primarily owing to the influence of the Coulomb barrier. Additionally, for the synthesis of the predicted double-magic nucleus ^{304}120, the maximal ER cross section is predicted to be 0.046 fb for the reaction $^{58}\mathrm{V} + {}^{249}\mathrm{Bk} \to {}^{304}120 + 3\mathrm{n}$, necessitating further development in both experimental techniques and reaction mechanisms.

Author contributions All authors contributed to the study conception and design. Material preparation, data collection and analysis were performed by Ming-Hao Zhang, Ying Zou, Mei-Chen Wang, Gen Zhang, Qing-Lin Niu and Feng-Shou Zhang. The first draft of the manuscript was written by Ming-Hao Zhang, and all authors commented on previous versions of the manuscript. All authors read and approved the final manuscript.

Data availability The data that support the findings of this study are openly available in Science Data Bank at https://cstr.cn/31253.11.sciencedb.j00186.00236 and https://doi.org/10.57760/sciencedb.j00186.00236.

Declarations

Conflict of interest Feng-Shou Zhang is an editorial board member for Nuclear Science and Techniques and was not involved in the editorial review, or the decision to publish this article. All authors declare that there are no conflict of interest.

References

1. P. Möller, A. Sierk, T. Ichikawa et al., Nuclear ground-state masses and deformations: FRDM (2012). At. Data. Nucl. Data Tables **109–110**, 1–204 (2016). https://doi.org/10.1016/j.adt.2015.10.002
2. S.G. Nilsson, C.F. Tsang, A. Sobiczewski et al., On the nuclear structure and stability of heavy and superheavy elements. Nucl. Phys. A **131**, 1–66 (1969). https://doi.org/10.1016/0375-9474(69)90809-4
3. S. Ćwiok, J. Dobaczewski, P.H. Heenen et al., Shell structure of the superheavy elements. Nucl. Phys. A **611**, 211–246 (1996). https://doi.org/10.1016/S0375-9474(96)00337-5
4. S. Ćwiok, P.H. Heenen, W. Nazarewicz, Shape coexistence and triaxiality in the superheavy nuclei. Nature **433**, 705–709 (2005). https://doi.org/10.1038/nature03336
5. D. Ackermann, C. Theisen, Nuclear structure features of very heavy and superheavy nuclei-tracing quantum mechanics towards the 'island of stability'. Phys. Scr. **92**, 083002 (2017). https://doi.org/10.1088/1402-4896/aa7921
6. K. Rutz, M. Bender, T. Bürvenich et al., Superheavy nuclei in self-consistent nuclear calculations. Phys. Rev. C **56**, 238–243 (1997). https://doi.org/10.1103/PhysRevC.56.238
7. A.T. Kruppa, M. Bender, W. Nazarewicz, P.G. Reinhard, T. Vertse, S. Ćwiok, Shell corrections of superheavy nuclei in self-consistent calculations. Phys. Rev. C **61**, 034313 (2000). https://doi.org/10.1103/PhysRevC.61.034313
8. J.X. Li, W.X. Wang, H.F. Zhang, Properties and synthesis of the superheavy nucleus $^{298}_{114}$Fl. Phys. Rev. C **106**, 044601 (2022). https://doi.org/10.1103/PhysRevC.106.044601
9. Y.Q. Xin, N.N. Ma, J.G. Deng et al., Properties of $Z = 114$ superheavy nuclei. Nucl. Sci. Tech. **32**, 55 (2021). https://doi.org/10.1007/s41365-021-00899-7
10. A. Sobiczewski, K. Pomorski, Description of structure and properties of superheavy nuclei. Prog. Part. Nucl. Phys. **58**, 292–349 (2007). https://doi.org/10.1016/j.ppnp.2006.05.001
11. M. Ismail, A.Y. Ellithi, A. Adel, H. Anwer, On magic numbers for super- and ultraheavy systems and hypothetical spherical double-magic nuclei. J. Phys. G Nucl. Part. Phys. **43**, 015101 (2015). https://doi.org/10.1088/0954-3899/43/1/015101
12. B.S. Cai, C.X. Yuan, Random forest-based prediction of decay modes and half-lives of superheavy nuclei. Nucl. Sci. Tech. **34**, 204 (2023). https://doi.org/10.1007/s41365-023-01354-5
13. Z. Wang, Z.Z. Ren, Predictions of the decay properties of the superheavy nuclei ^{293,294}119 and ^{294,295}120. Nucl. Tech. **46**, 080011 (2023). https://doi.org/10.11889/j.0253-3219.2023.hjs.46.080011. **(in Chinese)**
14. G. Münzenberg, S. Hofmann, F.P. Heßberger et al., Identification of element 107 by α correlation chains. Z. Phys. A **300**, 107–108 (1981). https://doi.org/10.1007/BF01412623
15. G. Münzenberg, P. Armbruster, H. Folger et al., The identification of element 108. Z. Phys. A **317**, 235–236 (1984). https://doi.org/10.1007/BF01421260
16. G. Münzenberg, P. Armbruster, F.P. Heßberger et al., Observation of one correlated α-decay in the reaction ^{58}Fe on $^{209}\mathrm{Bi} \to {}^{267}109$. Z. Phys. A Hadrons Nucl. **309**, 89–90 (1982). https://doi.org/10.1007/BF01420157

17. S. Hofmann, V. Ninov, F.P. Heßberger et al., Production and decay of ^{269}110. Z. Phys. A Hadrons Nucl. **350**(4), 277–280 (1995). https://doi.org/10.1007/BF01291181
18. S. Hofmann, V. Ninov, F.P. Heßberger et al., The new element 111. Z. Phys. A Hadrons Nucl. **350**, 281–282 (1995). https://doi.org/10.1007/BF01291182
19. S. Hofmann, V. Ninov, F.P. Heßberger et al., The new element 112. Z. Phys. A Hadrons Nucl. **354**, 229–230 (1996). https://doi.org/10.1007/BF02769517
20. K. Morita, K. Morimoto, D. Kaji et al., Experiment on the synthesis of element 113 in the reaction ^{209}Bi(^{70}Zn, n)^{278}113. J. Phys. Soc. Jpn. **73**, 2593–2596 (2004). https://doi.org/10.1143/jpsj.73.2593
21. Y.T. Oganessian, V.K. Utyonkov, Y.V. Lobanov et al., Synthesis of the isotopes of elements 118 and 116 in the ^{249}Cf and ^{245}Cm +^{48} Ca fusion reactions. Phys. Rev. C **74**, 044602 (2006). https://doi.org/10.1103/PhysRevC.74.044602
22. Y.T. Oganessian, A. Yeremin, A. Popeko et al., Synthesis of nuclei of the superheavy element 114 in reactions induced by ^{48}Ca. Nature **400**, 242 (1999). https://doi.org/10.1038/22281
23. Y.T. Oganessian, F.S. Abdullin, S.N. Dmitriev et al., Investigation of the ^{243}Am+ ^{48} Ca reaction products previously observed in the experiments on elements 113, 115, and 117. Phys. Rev. C **87**, 014302 (2013). https://doi.org/10.1103/PhysRevC.87.014302
24. Y.T. Oganessian, V.K. Utyonkov, Y.V. Lobanov et al., Observation of the decay of ^{292}116. Phys. Rev. C **63**, 011301(R) (2000). https://doi.org/10.1103/PhysRevC.63.011301
25. Y.T. Oganessian, F.S. Abdullin, P.D. Bailey et al., Synthesis of a new element with atomic number $Z = 117$. Phys. Rev. Lett. **104**, 142502 (2010). https://doi.org/10.1103/PhysRevLett.104.142502
26. T. Huang, D. Seweryniak, B.B. Back et al., Discovery of the new isotope ^{251}Lr: Impact of the hexacontetrapole deformation on single-proton orbital energies near the $Z = 100$ deformed shell gap. Phys. Rev. C **106**, L061301 (2022). https://doi.org/10.1103/PhysRevC.106.L061301
27. K. Morita, K. Morimoto, D. Kaji et al., Experiment on the synthesis of element 113 in the reaction ^{209}Bi (^{70}Zn, n) ^{278}113. J. Phys. Soc. Jpn. **73**, 2593 (2004). https://doi.org/10.1143/jpsj.73.2593
28. Y.T. Oganessian, V.K. Utyonkov, Super-heavy element research. Rep. Prog. Phys. **78**, 036301 (2015). https://doi.org/10.1088/0034-4885/78/3/036301
29. Y. Oganessian, V. Utyonkov, Superheavy nuclei from ^{48}Ca-induced reactions. Nucl. Phys. A **944**, 62–98 (2015). https://doi.org/10.1016/j.nuclphysa.2015.07.003
30. M. Thoennessen, Discovery of isotopes of elements with $Z \geq 100$. At. Data. Nucl. Data Tables **99**, 312–344 (2013). https://doi.org/10.1016/j.adt.2012.03.003
31. Z.Y. Zhang, Z.G. Gan, L. Ma et al., Observation of the superheavy nuclide ^{271}Ds. Chin. Phys. Lett. **29**, 012502 (2012). https://doi.org/10.1088/0256-307X/29/1/012502
32. Y.T. Oganessian, V.K. Utyonkov, M.V. Shumeiko et al., New isotope ^{276}Ds and its decay products ^{272}Hs and ^{268}Sg from the ^{232}Th +^{48} Ca reaction. Phys. Rev. C **108**, 024611 (2023). https://doi.org/10.1103/PhysRevC.108.024611
33. S. Hofmann, Synthesis of superheavy elements by cold fusion. Radiochim. Acta **99**, 405–428 (2011). https://doi.org/10.1524/ract.2011.1854
34. Y. Yano, The RIKEN RI beam factory project: a status report. Nucl. Instrum. Meth. B **261**, 1009–1013 (2007). https://doi.org/10.1016/j.nimb.2007.04.174
35. L.J. Mao, J.C. Yang, W.Q. Yang et al., Introduction of the Heavy Ion Research Facility in Lanzhou (HIRFL). J. Instrum. **15**, T12015 (2020). https://doi.org/10.1088/1748-0221/15/12/T12015
36. P. Ostroumov, M. Hausmann, K. Fukushima et al., Heavy ion beam physics at Facility for Rare Isotope Beams. J. Instrum. **15**, P12034 (2020). https://doi.org/10.1088/1748-0221/15/12/P12034
37. P. Dolegieviez, R. Ferdinand, X. Ledoux et al., Status of the SPIRAL2 Project, in *Proceedings of the 10th International Particle Accelerator Conference (IPAC'19)*, pp. 844–847 (2019). https://doi.org/10.18429/JACoW-IPAC2019-MOPTS005
38. W. Loveland, Synthesis of transactinide nuclei using radioactive beams. Phys. Rev. C **76**, 014612 (2007). https://doi.org/10.1103/PhysRevC.76.014612
39. K. Siwek-Wilczyńska, T. Cap, M. Kowal et al., Predictions of the fusion-by-diffusion model for the synthesis cross sections of Z = 114–120 elements based on macroscopic–microscopic fission barriers. Phys. Rev. C **86**, 014611 (2012). https://doi.org/10.1103/PhysRevC.86.014611
40. L. Liu, C.W. Shen, Q.F. Li et al., Residue cross sections of ^{50} Ti-induced fusion reactions based on the two-step model. Eur. Phys. J. A **52**, 35–39 (2016). https://doi.org/10.1140/epja/i2016-16035-0
41. C.W. Shen, Y. Abe, D. Boilley et al., Isospin dependence of reactions ^{48}Ca+$^{243-251}$Bk. Int. J. Mod. Phys. E **17**, 66–79 (2008). https://doi.org/10.1142/S0218301308011768
42. D. Boilley, Y. Abe, B. Cauchois et al., Elimination of fast variables and initial slip: a new mechanism for fusion hindrance in heavy-ion collisions. J. Phys. G Nucl. Part. Phys **46**, 115102 (2019). https://doi.org/10.1088/1361-6471/ab11ef
43. V. Zagrebaev, W. Greiner, Cross sections for the production of superheavy nuclei. Nucl. Phys. A **944**, 257–307 (2015). https://doi.org/10.1016/j.nuclphysa.2015.02.010. (**Special Issue on Superheavy Elements**)
44. S. Amano, Y. Aritomo, M. Ohta, Dynamical mechanism of fusion hindrance in heavy ion collisions. Phys. Rev. C **108**, 014612 (2023). https://doi.org/10.1103/PhysRevC.108.014612
45. Y. Aritomo, Possibility of synthesizing a doubly magic superheavy nucleus. Phys. Rev. C. **75**, 024602 (2007). https://doi.org/10.1103/PhysRevC.75.024602
46. N. Wang, Z. Li, X. Wu, Improved quantum molecular dynamics model and its applications to fusion reaction near barrier. Phys. Rev. C **65**, 064608 (2002). https://doi.org/10.1103/PhysRevC.65.064608
47. L.L. Zhou, J.J. Cai, L.Q. Li et al., Fusion enhancement in the collisions with ^{44}Ca beams and the production of neutron-deficient $^{245-250}$Lr isotopes. Phys. Rev. C **109**, 024606 (2024). https://doi.org/10.1103/PhysRevC.109.024606
48. P. McGlynn, C. Simenel, Time-dependent Hartree–Fock study of quasifission trajectories in reactions forming ^{294}Og. Phys. Rev. C **107**, 054614 (2023). https://doi.org/10.1103/PhysRevC.107.054614
49. X.X. Sun, L. Guo, Microscopic study of the hot-fusion reaction ^{48}Ca +^{238} U with the constraints from time-dependent Hartree–Fock theory. Phys. Rev. C **107**, 064609 (2023). https://doi.org/10.1103/PhysRevC.107.064609
50. A.S. Umar, V.E. Oberacker, J.A. Maruhn et al., Entrance channel dynamics of hot and cold fusion reactions leading to superheavy elements. Phys. Rev. C **81**, 064607 (2010). https://doi.org/10.1103/PhysRevC.81.064607
51. K. Sekizawa, K. Hagino, Time-dependent Hartree–Fock plus Langevin approach for hot fusion reactions to synthesize the $Z = 120$ superheavy element. Phys. Rev. C **99**, 051602(R) (2019). https://doi.org/10.1103/PhysRevC.99.051602
52. R. Gumbel, C. Ross, A.S. Umar, Role of isospin composition in low-energy nuclear fusion. Phys. Rev. C **108**, L051602 (2023). https://doi.org/10.1103/PhysRevC.108.L051602

53. Y.H. Zhang, J.J. Li, C. Li et al., Microscopic study of the production of neutron-rich isotopes near $N = 126$ in the multinucleon transfer reactions ^{78,82,86}Kr $+^{208}$ Pb. Phys. Rev. C. **109**, 044617 (2024). https://doi.org/10.1103/PhysRevC.109.044617
54. Z.P. Gao, Y.N. Zhang, L. Zhu et al., Role of the isospin diffusion on the cluster transfer in ^{12,14}C $+^{209}$ Bi reactions. Phys. Rev. C. **109**, L041605 (2024). https://doi.org/10.1103/PhysRevC.109.L041605
55. N. Wang, E.G. Zhao, W. Scheid et al., Theoretical study of the synthesis of superheavy nuclei with $Z = 119$ and 120 in heavy-ion reactions with trans-uranium targets. Phys. Rev. C **85**, 041601 (2012). https://doi.org/10.1103/PhysRevC.85.041601
56. J. Hong, G. Adamian, N. Antonenko et al., Possibilities of direct production of superheavy nuclei with $Z = 112$–118 in different evaporation channels. Phys. Lett. B **809**, 135760 (2020). https://doi.org/10.1016/j.physletb.2020.135760
57. S.Q. Guo, X.J. Bao, H.F. Zhang et al., Effect of dynamical deformation on the production distribution in multinucleon transfer reactions. Phys. Rev. C **100**, 054616 (2019). https://doi.org/10.1103/PhysRevC.100.054616
58. Z.Q. Feng, G.M. Jin, F. Fu et al., Production cross sections of superheavy nuclei based on dinuclear system model. Nucl. Phys. A **771**, 50–67 (2006). https://doi.org/10.1016/j.nuclphysa.2006.03.002
59. Z.H. Wu, L. Zhu, F. Li et al., Synthesis of neutron-rich superheavy nuclei with radioactive beams within the dinuclear system model. Phys. Rev. C **97**, 064609 (2018). https://doi.org/10.1103/PhysRevC.97.064609
60. S.H. Zhu, X.J. Bao, Possibility to synthesize $Z = 120$ superheavy nuclei with $Z > 20$ projectiles. Phys. Rev. C **108**, 014604 (2023). https://doi.org/10.1103/PhysRevC.108.014604
61. M.H. Zhang, Y.H. Zhang, Y. Zou et al., Predictions of synthesizing elements with $Z = 119$ and 120 in fusion reactions. Phys. Rev. C **109**, 014622 (2024). https://doi.org/10.1103/PhysRevC.109.014622
62. J.J. Li, N. Tang, Y.H. Zhang et al., Progress on production cross-sections of unknown nuclei in fusion evaporation reactions and multinucleon transfer reactions. Int. J. Mod. Phys. E **32**, 2330002 (2023). https://doi.org/10.1142/S0218301323300023
63. A. Nasirov, B. Kayumov, Optimal colliding energy for the synthesis of a superheavy element with $Z = 119$. Phys. Rev. C **109**, 024613 (2024). https://doi.org/10.1103/PhysRevC.109.024613
64. L. Reddi Rani, N. Sowmya, H.C. Manjunatha, K.N. Sridhar, M.M. Armstrong Arasu, Optimal incident energy of heavy ion fusion. Phys. Rev. C **109**, 024610 (2024). https://doi.org/10.1103/PhysRevC.109.024610
65. L.Q. Li, G. Zhang, F.S. Zhang, Production of unknown Fl isotopes in proton evaporation channels within the dinuclear system model. Phys. Rev. C **106**, 024601 (2022). https://doi.org/10.1103/PhysRevC.106.024601
66. X.J. Bao, Y. Gao, J.Q. Li et al., Theoretical study of the synthesis of superheavy nuclei using radioactive beams. Phys. Rev. C **91**, 064612 (2015). https://doi.org/10.1103/PhysRevC.91.064612
67. L. Zhu, J. Su, C. Li et al., How to approach the island of stability: Reactions using multinucleon transfer or radioactive neutron-rich beams? Phys. Lett. B **829**, 137113 (2022). https://doi.org/10.1016/j.physletb.2022.137113
68. X.B. Yu, L. Zhu, Z.H. Wu et al., Predictions for production of superheavy nuclei with $Z = 105$–112 in hot fusion reactions. Nucl. Sci. Tech. **29**, 154 (2018). https://doi.org/10.1007/s41365-018-0501-2
69. P.H. Chen, H. Wu, Z.X. Yang et al., Prediction of synthesis cross sections of new moscovium isotopes in fusion-evaporation reactions. Nucl. Sci. Tech. **34**, 7 (2023). https://doi.org/10.1007/s41365-022-01157-0
70. C. Li, P.W. Wen, J.J. Li et al., Production of heavy neutron-rich nuclei with radioactive beams in multinucleon transfer reactions. Nucl. Sci. Tech. **28**, 110 (2017). https://doi.org/10.1007/s41365-017-0266-z
71. M.H. Zhang, Y.H. Zhang, J.J. Li et al., Progress in transport models of heavy-ion collisions for the synthesis of superheavy nuclei. Nucl. Tech. **46**, 080014 (2023). https://doi.org/10.11889/j.0253-3219.2023.hjs.46.080014. (**in Chinese**)
72. P.H. Chen, C. Geng, Z.X. Yang et al., Production of neutron-rich actinide isotopes in isobaric collisions via multinucleon transfer reactions. Nucl. Sci. Tech. **34**, 160 (2023). https://doi.org/10.1007/s41365-023-01314-z
73. Z.H. Liao, L. Zhu, Z.P. Gao et al., Optimal detection angles for producing $N = 126$ neutron-rich isotones in multinucleon transfer reactions. Phys. Rev. Res. **5**, L022021 (2023). https://doi.org/10.1103/PhysRevResearch.5.L022021
74. M.H. Zhang, Y.H. Zhang, Y. Zou et al., Possibilities for the synthesis of superheavy element $Z = 121$ in fusion reactions. Nucl. Sci. Tech. **35**, 95 (2024). https://doi.org/10.1007/s41365-024-01452-y
75. V.I. Zagrebaev, Synthesis of superheavy nuclei: nucleon collectivization as a mechanism for compound nucleus formation. Phys. Rev. C **64**, 034606 (2001). https://doi.org/10.1103/PhysRevC.64.034606
76. A.S. Zubov, G.G. Adamian, N.V. Antonenko et al., Survival probability of superheavy nuclei. Phys. Rev. C **65**, 024308 (2002). https://doi.org/10.1103/PhysRevC.65.024308
77. Z. Ahmed, Tunnelling through the Morse barrier. Phys. Lett. A **157**, 1–5 (1991). https://doi.org/10.1016/0375-9601(91)90399-S
78. V.Y. Denisov, Expression for the heavy-ion fusion cross section. Phys. Rev. C **107**, 054618 (2023). https://doi.org/10.1103/PhysRevC.107.054618
79. S. Rana, R. Kumar, S. Patra et al., Fusion dynamics of astrophysical reactions using different transmission coefficients. Eur. Phys. J. A **58**, 241 (2022). https://doi.org/10.1140/epja/s10050-022-00893-6
80. B. Wang, K. Wen, W.J. Zhao et al., Systematics of capture and fusion dynamics in heavy-ion collisions. At. Data Nucl. Data Tables **114**, 281–370 (2017). https://doi.org/10.1016/j.adt.2016.06.003
81. W.D. Myers, W.J. Swiatecki, Nuclear masses and deformations. Nucl. Phys. **81**, 1–60 (1966). https://doi.org/10.1016/0029-5582(66)90639-0
82. C.Y. Wong, Interaction barrier in charged-particle nuclear reactions. Phys. Rev. Lett. **31**, 766–769 (1973). https://doi.org/10.1103/PhysRevLett.31.766
83. G.G. Adamian, N.V. Antonenko, R.V. Jolos et al., Effective nucleus–nucleus potential for calculation of potential energy of a dinuclear system. Int. J. Mod. Phys. E **5**, 191 (1996). https://doi.org/10.1142/S0218301396000098
84. S. Ayik, B. Schürmann, W. Nörenberg, Microscopic transport theory of heavy-ion collisions. Z. Phys. A **277**, 299–310 (1976). https://doi.org/10.1007/BF01415605
85. G.G. Adamian, N.V. Antonenko, W. Scheid, Characteristics of quasifission products within the dinuclear system model. Phys. Rev. C **68**, 034601 (2003). https://doi.org/10.1103/PhysRevC.68.034601
86. N. Wang, L. Dou, E.G. Zhao et al., Nuclear hexadecapole deformation effects on the production of super-heavy elements. Chin. Phys. Lett. **27**, 062502 (2010). https://doi.org/10.1088/0256-307X/27/6/062502
87. J.Q. Li, G. Wolschin, Distribution of the dissipated angular momentum in heavy-ion collisions. Phys. Rev. C **27**, 590–601 (1983). https://doi.org/10.1103/PhysRevC.27.590

88. J.D. Jackson, A schematic model for (p, xn) cross sections in heavy elements. Can. J. Phys. **34**, 767–779 (1956). https://doi.org/10.1139/p56-087
89. V. Weisskopf, Statistics and nuclear reactions. Phys. Rev. **52**, 295–303 (1937). https://doi.org/10.1103/PhysRev.52.295
90. N. Bohr, J.A. Wheeler, The mechanism of nuclear fission. Phys. Rev. **56**, 426–450 (1939). https://doi.org/10.1103/PhysRev.56.426
91. L. Zhu, Selection of projectiles for producing trans-uranium nuclei in transfer reactions within the improved dinuclear system model. J. Phys. G Nucl. Part. Phys **47**, 065107 (2020). https://doi.org/10.1088/1361-6471/ab871f
92. H.L. Lü, D. Boilley, Y. Abe et al., Synthesis of superheavy elements: uncertainty analysis to improve the predictive power of reaction models. Phys. Rev. C **94**, 034616 (2016). https://doi.org/10.1103/PhysRevC.94.034616
93. J.A. Sheikh, W. Nazarewicz, J.C. Pei, Systematic study of fission barriers of excited superheavy nuclei. Phys. Rev. C **80**, 011302(R) (2009). https://doi.org/10.1103/PhysRevC.80.011302
94. W.F. Li, Z.Z. Wang, H.S. Xu et al., Odd-even effects of the survival probability for superheavy compound nuclei. Chin. Phys. Lett. **21**, 636 (2004). https://doi.org/10.1088/0256-307X/21/4/013
95. C.J. Xia, B.X. Sun, E.G. Zhao et al., Systematic study of survival probability of excited superheavy nuclei. Sci. China Phys. Mech. Astron. **54**, 109–113 (2011). https://doi.org/10.1007/s11433-011-4438-2
96. V.K. Utyonkov, N.T. Brewer, Y.T. Oganessian et al., Experiments on the synthesis of superheavy nuclei ^{284}Fl and ^{285}Fl in the ^{239,240}Pu $+^{48}$ Ca reactions. Phys. Rev. C **92**, 034609 (2015). https://doi.org/10.1103/PhysRevC.92.034609
97. V.K. Utyonkov, N.T. Brewer, Y.T. Oganessian et al., Neutron-deficient superheavy nuclei obtained in the ^{240}Pu $+^{48}$ Ca reaction. Phys. Rev. C **97**, 014320 (2018). https://doi.org/10.1103/PhysRevC.97.014320
98. Y.T. Oganessian, V.K. Utyonkov, Y.V. Lobanov et al., Measurements of cross sections and decay properties of the isotopes of elements 112, 114, and 116 produced in the fusion reactions ^{233,238}U,^{242} Pu, and ^{248}Cm $+^{48}$ Ca. Phy. Rev. C **70**(6), 064609 (2004). https://doi.org/10.1103/PhysRevC.70.064609
99. Y.T. Oganessian, V.K. Utyonkov, D. Ibadullayev et al., Investigation of ^{48}Ca-induced reactions with ^{242}Pu and ^{238}U targets at the JINR superheavy element factory. Phys. Rev. C **106**, 024612 (2022). https://doi.org/10.1103/PhysRevC.106.024612
100. Y.T. Oganessian, V.K. Utyonkov, Y.V. Lobanov et al., Measurements of cross sections for the fusion-evaporation reactions $^{244}\mathrm{Pu}(^{48}\mathrm{Ca}, xn)^{292-x}114$ and $^{245}\mathrm{Cm}(^{48}\mathrm{Ca}, xn)^{293-x}116$. Phys. Rev. C **69**, 054607 (2004). https://doi.org/10.1103/PhysRevC.69.054607
101. L. Stavsetra, K.E. Gregorich, J. Dvorak et al., Independent verification of element 114 production in the ^{48}Ca+^{242}Pu reaction. Phys. Rev. Lett. **103**, 132502 (2009). https://doi.org/10.1103/PhysRevLett.103.132502
102. P.A. Ellison, K.E. Gregorich, J.S. Berryman et al., New superheavy element isotopes: $^{242}\mathrm{Pu}(^{48}\mathrm{Ca}, 5n)^{285}114$. Phys. Rev. Lett. **105**, 182701 (2010). https://doi.org/10.1103/PhysRevLett.105.182701
103. J.M. Gates, C.E. Düllmann, M. Schädel et al., First superheavy element experiments at the GSI recoil separator TASCA: the production and decay of element 114 in the $^{244}\mathrm{Pu}(^{48}\mathrm{Ca},3\text{–}4n)$ reaction. Phys. Rev. C **83**, 054618 (2011). https://doi.org/10.1103/PhysRevC.83.054618
104. E.M. Kozulin, G.N. Knyazheva, I.M. Itkis et al., Fusion–fission and quasifission of superheavy systems with $Z = 110$–116 formed in ^{48}Ca-induced reactions. Phys. Rev. C **90**, 054608 (2014). https://doi.org/10.1103/PhysRevC.90.054608

Springer Nature or its licensor (e.g. a society or other partner) holds exclusive rights to this article under a publishing agreement with the author(s) or other rightsholder(s); author self-archiving of the accepted manuscript version of this article is solely governed by the terms of such publishing agreement and applicable law.